

Complex networks derived from cellular automata

Yoshihiko Kayama

*Department of Media and Information, BAIKA Women's University,
2-19-5, Shukuno-sho, Ibaraki-city, Osaka-pref., Japan*

Abstract

We propose a method for deriving networks from one-dimensional binary cellular automata. The derived networks are usually directed and have structural properties corresponding to the dynamical behaviors of their cellular automata. Network parameters, particularly the efficiency and the degree distribution, show that the dependence of efficiency on the grid size is characteristic and can be used to classify cellular automata and that derived networks exhibit various degree distributions. In particular, a class IV rule of Wolfram's classification produces a network having a scale-free distribution.

Keywords: complex networks, cellular automata, scale-free, small-world

1. Introduction

Cellular automata (CA) have been used to study the critical phenomena of complex systems. S. Wolfram has systematically investigated the dynamical behavior of one-dimensional automata and identified the following four essential types: homogeneous (class I), periodic (class II), chaotic (class III), and complex (class IV) [1]. In particular, class IV rules produce complex structures with long transients. Alternatively, complex networks exhibiting a scale-free topology can be identified ubiquitously; for example, they occur in social relationships [2], biological and chemical systems [3, 4], and the Internet [5, 6]. Such networks have been studied extensively in the wake of papers by Watts and Strogatz on small-world networks [7] and by Barabási and Albert on scale-free networks [8]. Even though both CA and complex networks are used to study complex systems and various phenomena, their relation is not clear.

In recent years, the dynamics of Boolean networks with complex topology have been studied [9]-[13] yielding several notable results such as the dependence of dynamical phases on network topology [10] and the robustness of scale-free networks [11]. Our approach is to define networks that correspond to the dynamical behaviors of CA.

In this article, we propose a method for deriving networks from the time evolution of CA configurations. For transformations of the CA rule function, the adjacency matrix of the network exhibits characteristic properties. We investigate networks derived from the typical rules of one-dimensional binary CA with three and five neighbors. Our studies reveal that the *structural* properties of the derived network reflect the *dynamical* behaviors of the CA rule and that chaotic or critical rules lead to complex network topologies. We use two parameters to characterize the topology of such networks: the efficiency of the network (corresponding to the harmonic mean of its shortest path lengths) and its degree distribution. The efficiency shows a characteristic scale dependence on the grid size of the cellular automaton and may be useful in classifying CA rules. Class III rules correspond to random networks, and a scale-free degree distribution has been obtained from the class IV rule.

The next section describes our notation and some definitions relevant to CA. In section 3, we describe our method for deriving networks from CA rules and discuss their properties under transformations of the CA rule function. Section 4 reports on the efficiency and degree distribution of derived networks and discusses the correspondence between the dynamical behavior of a cellular automaton and the structural properties of its derived network.

2. Notation and definitions relevant to cellular automata

CA are dynamical systems that consist of a regular grid of cells, each characterized by a finite number of states. CA are updated synchronously in discrete time steps according to a local rule (CA rule) that

Email address: kayama@baika.ac.jp (Yoshihiko Kayama)

is identical at every cell. In a one-dimensional grid, each cell is connected to its r local neighbors on either side, where r is referred to as the *radius*. Thus, each cell has $2r + 1$ neighbors, including itself. The state of a cell for the next time step is determined from the current states of the neighboring cells: $x_i(t + 1) = f(x_{i-r}(t), \dots, x_i(t), \dots, x_{i+r}(t))$, where $x_i(t)$ denotes the state of cell i at time t , and f is the transition rule function. The term *configuration* refers to an assignment of states to all the cells for a given time step; a configuration is denoted by $\mathbf{x}(t) = (x_0(t), x_1(t), \dots, x_{N-1}(t))$, where N is the grid size. Thus, the time transition of a configuration $\mathbf{x}(t)$ with periodic boundary conditions is given by

$$\mathbf{x}(t + 1) = \mathbf{f}(\mathbf{x}(t)) \quad (1)$$

$$\begin{aligned} &= (f(x_{N-r}(t), \dots, x_0(t), \dots, x_r(t)), \\ &\quad f(x_{N-r+1}(t), \dots, x_1(t), \dots, x_{1+r}(t)), \\ &\quad \dots, f(x_{N-1-r}(t), \dots, x_{N-1}(t), \dots, x_{r-1}(t))), \end{aligned} \quad (2)$$

where \mathbf{f} represents a mapping on the configuration space $\{\mathbf{x}\}_N$. In this article, we restrict our discussion to *binary* CA, which satisfy $x_i \in \{0, 1\}$ for all i .

For a given configuration \mathbf{x} , the mirror (left-right reflection) and complement (0-1 exchange) configurations are denoted as $\tilde{\mathbf{x}} \equiv (x_{N-1}, \dots, x_1, x_0)$ and $\bar{\mathbf{x}} \equiv (\bar{x}_0, \bar{x}_1, \dots, \bar{x}_{N-1})$, respectively. By analogy, the mirror, complement and mirror-complement of a rule function f are defined as follows:

$$\tilde{f}(x_{i-r}, \dots, x_i, \dots, x_{i+r}) \equiv \frac{f(x_{i+r}, \dots, x_i, \dots, x_{i-r})}{f(x_{i-r}, \dots, x_i, \dots, x_{i+r})} \quad (3)$$

$$\bar{f}(x_{i-r}, \dots, x_i, \dots, x_{i+r}) \equiv \frac{f(\bar{x}_{i+r}, \dots, \bar{x}_i, \dots, \bar{x}_{i-r})}{f(\bar{x}_{i-r}, \dots, \bar{x}_i, \dots, \bar{x}_{i+r})} \quad (4)$$

$$\tilde{\bar{f}}(x_{i-r}, \dots, x_i, \dots, x_{i+r}) \equiv \frac{f(\bar{x}_{i+r}, \dots, \bar{x}_i, \dots, \bar{x}_{i-r})}{f(\bar{x}_{i+r}, \dots, \bar{x}_i, \dots, \bar{x}_{i-r})} \quad (5)$$

respectively. The CA rules of these transformed functions are equivalent to the original rule f [14]. It is trivial that mirror and complement operations are commutative, i.e. $\tilde{\bar{f}} = \bar{\tilde{f}}$. The mappings defined from these functions are

$$\begin{aligned} \tilde{\mathbf{f}}(\mathbf{x}) &\equiv (\tilde{f}(x_{N-r}, \dots, x_0, \dots, x_r), \tilde{f}(x_{N-r+1}, \dots, x_1, \dots, x_{1+r}), \\ &\quad \dots, \tilde{f}(x_{N-1-r}, \dots, x_{N-1}, \dots, x_{r-1})) \end{aligned} \quad (6)$$

$$\begin{aligned} &= (f(x_r, \dots, x_0, \dots, x_{N-r}), f(x_{1+r}, \dots, x_1, \dots, x_{N-r+1}), \\ &\quad \dots, f(x_{r-1}, \dots, x_{N-1}, \dots, x_{N-1-r})) \end{aligned} \quad (7)$$

$$= \mathbf{f}(\tilde{\mathbf{x}}) \quad (8)$$

$$\begin{aligned} \bar{\mathbf{f}}(\mathbf{x}) &\equiv (\bar{f}(x_{N-r}, \dots, x_0, \dots, x_r), \bar{f}(x_{N-r+1}, \dots, x_1, \dots, x_{1+r}), \\ &\quad \dots, \bar{f}(x_{N-1-r}, \dots, x_{N-1}, \dots, x_{r-1})) \end{aligned} \quad (9)$$

$$\begin{aligned} &= (\bar{f}(\bar{x}_{N-r}, \dots, \bar{x}_0, \dots, \bar{x}_r), \bar{f}(\bar{x}_{N-r+1}, \dots, \bar{x}_1, \dots, \bar{x}_{1+r}), \\ &\quad \dots, \bar{f}(\bar{x}_{N-1-r}, \dots, \bar{x}_{N-1}, \dots, \bar{x}_{r-1})) \end{aligned} \quad (10)$$

$$= \overline{\mathbf{f}(\bar{\mathbf{x}})} \quad (11)$$

$$\tilde{\bar{\mathbf{f}}}(\mathbf{x}) = \overline{\mathbf{f}(\tilde{\mathbf{x}})} = \tilde{\mathbf{f}}(\mathbf{x}). \quad (12)$$

A t -fold repetition of these mappings yields, respectively,

$$\tilde{\mathbf{f}}^t(\mathbf{x}) = \overline{\mathbf{f}_R^t(\tilde{\mathbf{x}})} \quad (13)$$

$$\bar{\mathbf{f}}^t(\mathbf{x}) = \overline{\mathbf{f}_R^t(\bar{\mathbf{x}})} \quad (14)$$

$$\tilde{\bar{\mathbf{f}}}^t(\mathbf{x}) = \overline{\mathbf{f}_R^t(\tilde{\mathbf{x}})} = \tilde{\mathbf{f}}^t(\mathbf{x}). \quad (15)$$

Elementary Cellular Automata (ECA) are the simplest nontrivial binary CA; they are defined on a one-dimensional grid with minimal neighborhood size ($r = 1$). The $2^3 = 8$ different neighborhood configurations result in $2^8 = 256$ possible rules, of which 88 are nonequivalent under the transformations (3)-(5) [14]. ECA rules are generally referred to by their Wolfram code, a standard naming convention invented by Wolfram [1, 15] that gives each rule a number from 0 to 255. For example, rule 30 exhibits

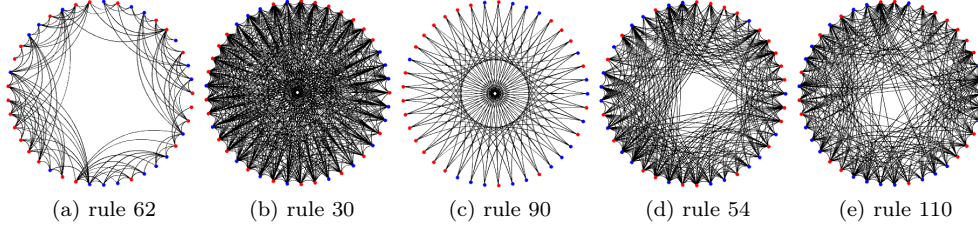


Figure 1: Examples of network graphs derived from ECA rules with $N = 41$ and $t = 20$. The dots on the circumference of each graph correspond to the nodes of the derived network, which in turn correspond to the cells of the cellular automaton. The time t is selected to give each cell causal relationships with all other cells and to avoid repetitions.

class III behavior, meaning that even simple input patterns lead to chaotic, seemingly random histories. Rule 90 is also chaotic with a fractal structure (Sierpinski triangle). Furthermore, rule 110 generates class IV behavior, which is neither completely random nor completely repetitive. Localized structures appear and interact in various complicated ways.

Other simple models are 5-neighbor ($r = 2$) CA, which contain 2^{32} rules. Our discussion is restricted to the *totalistic* CA (5TCA), in which the state of each cell at time t depends only on the sum of the states of the cells in its neighborhood at the previous time. Of the $2^6 = 64$ totalistic rules, 36 are independent. To avoid confusion, we add the letter “ T ” to the Wolfram code of the 5TCA rules, e.g., rule $T20$.

3. Derivation of networks from CA rules

We consider a one-dimensional grid with N cells, where each cell is connected to its r nearest neighbors with periodic boundary conditions. Each cell state $x \in \{0, 1\}$ evolves by an identical CA rule function f_R , where R denotes its Wolfram code. After t time steps, the configuration of cells obtained from an initial one $\varphi \equiv \mathbf{x}(0)$ is given by $\mathbf{x}(t, \varphi) = \mathbf{f}_R^t(\varphi)$. If φ_i denotes the initial configuration with a changed state for cell i , the difference between the configurations after t time steps from φ_i and φ can be written as

$$\Delta_i \mathbf{x}(t, \varphi) \equiv \mathbf{x}(t, \varphi_i) - \mathbf{x}(t, \varphi) \pmod{2} = \mathbf{f}_R^t(\varphi_i) - \mathbf{f}_R^t(\varphi) \pmod{2} \quad (16)$$

where $\Delta_i \mathbf{x}(t, \varphi)$ characterizes the influence of cell i on other cells in the grid after t time steps. This influence represents the flow of information from cell i through the network. We define a matrix as

$$A_R(t, \varphi) \equiv [\Delta_0 \mathbf{x}(t, \varphi), \Delta_1 \mathbf{x}(t, \varphi), \dots, \Delta_{N-1} \mathbf{x}(t, \varphi)]^T \quad (17)$$

$$= [\Delta_0 \mathbf{f}_R^t(\varphi), \Delta_1 \mathbf{f}_R^t(\varphi), \dots, \Delta_{N-1} \mathbf{f}_R^t(\varphi)]^T, \quad (18)$$

where the transpose operation T does not apply to the individual elements $\Delta_i \mathbf{x}(t, \varphi)$. We treat $A_R(t, \varphi)$ as the *adjacency matrix* of a network derived from the CA rule R ; an entry $a_{ij} = 1$ if a directed edge from node i to node j exists, and 0 otherwise. Because $\Delta_i \mathbf{x}(t, \varphi)$ depends on the initial configuration, $A_R(t, \varphi)$ gives a different network for each initial configuration. Although this derived network is not identical with an analogous network derived by considering the change of two or more cells, it captures essential properties of its cellular automaton, as shown below. Some graphs derived from ECA and 5TCA rules are presented in Fig.1 and Fig.2, respectively.

From Eqs.(13), (16) and (18), the adjacency matrix is transformed by the mirror operation as follows:

$$\begin{aligned} \tilde{A}_R(t, \varphi) &\equiv [\Delta_0 \tilde{\mathbf{f}}_R^t(\varphi), \Delta_1 \tilde{\mathbf{f}}_R^t(\varphi), \dots, \Delta_{N-1} \tilde{\mathbf{f}}_R^t(\varphi)]^T \\ &= [\Delta_{N-1} \tilde{\mathbf{f}}_R^t(\tilde{\varphi}), \Delta_{N-2} \tilde{\mathbf{f}}_R^t(\tilde{\varphi}), \dots, \Delta_0 \tilde{\mathbf{f}}_R^t(\tilde{\varphi})]^T \end{aligned} \quad (19)$$

$$= A_R(t, \tilde{\varphi}), \quad (20)$$

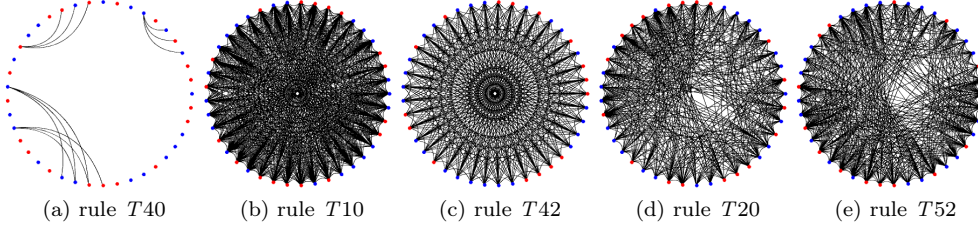


Figure 2: Examples of network graphs derived from 5TCA rules with $N = 41$ and $t = 10$.

where the subscript of Δ in Eq.(19) labels the state-changed elements of $\tilde{\varphi}$ and the \sim operation acting on the adjacency matrix in the right-hand side of Eq.(20) represents the mirroring of elements about both the horizontal and vertical axes. Similarly, the complement of the adjacency matrix is obtained from Eqs.(14), (16) and (18) as follows:

$$\begin{aligned}
\bar{A}_R(t, \varphi) &\equiv \left[\Delta_0 \bar{\mathbf{f}}_R^t(\varphi), \Delta_1 \bar{\mathbf{f}}_R^t(\varphi), \dots, \Delta_{N-1} \bar{\mathbf{f}}_R^t(\varphi) \right]^T \\
&= \left[\Delta_0 \overline{\mathbf{f}_R^t(\varphi)}, \Delta_1 \overline{\mathbf{f}_R^t(\varphi)}, \dots, \Delta_{N-1} \overline{\mathbf{f}_R^t(\varphi)} \right]^T \\
&= \left[\Delta_0 \mathbf{f}_R^t(\bar{\varphi}), \Delta_1 \mathbf{f}_R^t(\bar{\varphi}), \dots, \Delta_{N-1} \mathbf{f}_R^t(\bar{\varphi}) \right]^T \\
&= A_R(t, \bar{\varphi}),
\end{aligned} \tag{21}$$

$$= A_R(t, \bar{\varphi}), \tag{22}$$

where Eq.(21) is derived from the invariance of the *modulo* operation in Eq.(16) under complementation. In general, the graph of the complement $\bar{A}_R(t, \varphi)$ is not identical with the “graph complement” [16] of $A_R(t, \varphi)$. Finally, the mirror-complement of the adjacency matrix is

$$\bar{\bar{A}}_R(t, \varphi) = \widetilde{A_R(t, \bar{\varphi})} = \bar{\bar{A}}_R(t, \varphi). \tag{23}$$

An important property of the adjacency matrix may be derived for self-complementary rule functions. Adding the transformations (3)-(5), we define the *diminished-radix complement* of the rule function f_R as

$$\hat{f}_R(x_{i-r}, \dots, x_i, \dots, x_{i+r}) \equiv f_R(\bar{x}_{i-r}, \dots, \bar{x}_i, \dots, \bar{x}_{i+r}). \tag{24}$$

If a mapping \mathbf{f}_R is *self-complementary*, i.e. $\mathbf{f}_R = \bar{\mathbf{f}}_R$, the mapping $\hat{\mathbf{f}}_R^t$ obtained from \hat{f}_R satisfies the equation

$$\hat{\mathbf{f}}_R^t(\varphi) = \begin{cases} \overline{\mathbf{f}_R^t(\varphi)} & \text{for odd } t \\ \mathbf{f}_R^t(\varphi) & \text{for even } t. \end{cases} \tag{25}$$

Therefore, $\Delta_i \hat{\mathbf{f}}_R^t(\varphi)$ is equal to $\Delta_i \mathbf{f}_R^t(\varphi)$ for all t , and the adjacency matrix $\hat{A}_R(t, \varphi)$ defined by $\hat{\mathbf{f}}_R^t(\varphi)$ is identical with $A_R(t, \varphi)$. Although this property of the adjacency matrix makes the rule \hat{f}_R indistinguishable from rule R , this degeneracy is not a drawback of our method but rather a new way of detecting similarity among CA rules, as described below.

Another interesting property of our approach pertains to *additive mappings* which satisfy the equation $\mathbf{f}_R(\mathbf{x} + \mathbf{y} \pmod{2}) = \mathbf{f}_R(\mathbf{x}) + \mathbf{f}_R(\mathbf{y}) \pmod{2}$. Eq.(16) leads to the result $\Delta_i \mathbf{x}(t, \varphi) = \mathbf{f}_R^t(\mathbf{0}_i)$, where $\mathbf{0}_i$ is the *null* configuration except at cell i . Thus, the adjacency matrix (18) is independent of the initial configuration and all nodes of the derived network are equivalent. Hence, the same number of edges connects to each node. If an edge from node i to node j exists, an edge also exists in the opposite direction; the network is undirected, which means that the adjacency matrix is symmetric. For example, rule 90 is additive and, for this reason, corresponds to the geometrical graph shown in Fig.1(c). Furthermore, if cell

15(85)	240(170)
23	232
43(113)	212(142)
51	204
77	178
105	150

7	56
11	52
21	42
25	38

(a) ECA pairs

(b) 5TCA pairs

Table 1: The diminished-radix complements pairs of self-complement rules of ECA and 5TCA. The rule inside the parentheses is mirror equivalent to the one outside the parentheses.

i and cell j change their states in the initial configuration φ , the difference between the configurations φ_{ij} and φ after t time steps satisfies the equation

$$\begin{aligned}
\Delta_{ij}\mathbf{x}(t, \varphi) &= \mathbf{f}_R^t(\varphi_{ij}) + \mathbf{f}_R^t(\varphi) \pmod{2} = \mathbf{f}_R^t(\mathbf{0}_{ij}) = \mathbf{f}_R^t(\mathbf{0}_i) + \mathbf{f}_R^t(\mathbf{0}_j) \pmod{2} \\
&= \Delta_i\mathbf{x}(t, \mathbf{0}) + \Delta_j\mathbf{x}(t, \mathbf{0}) \pmod{2} \\
&= (A_R(t))_i + (A_R(t))_j \pmod{2}.
\end{aligned} \tag{26}$$

where $(A)_i$ denotes i -th row vector of matrix A . Consequently, the adjacency matrix for additive mappings can represent the influence of changes at more than two cells.

4. Properties of derived networks

Following the Wolfram's classification, we examine some typical rules of ECA and 5TCA. There is no reason to restrict our discussion to even-numbered rules. We use two basic parameters, the efficiency and the degree distribution, to investigate the properties and complexities of derived networks.

A descriptive network parameter is the distribution of degrees. $P_R(k_{in})$ and $P_R(k_{out})$ indicate the probabilities of a node having an in-degree k_{in} and an out-degree k_{out} , respectively. In particular, scale-free networks are the class of networks whose degree distribution is a power-law: $P(k) \sim k^{-\gamma}$, where γ is called the *scale-free exponent*. Small-world networks can be categorized by their average shortest path length $l = \langle d_{ij} \rangle$, where d_{ij} is the length of the shortest path between node i and node j . To sidestep any divergence of the d_{ij} , we consider their harmonic mean, which we use to define the network efficiency $E = \frac{1}{N(N-1)} \sum_{i \neq j} \frac{1}{d_{ij}}$ [17, 18].

Because these parameters are calculated for adjacency matrices obtained from randomly generated initial configurations, the transformed matrices defined in Eqs.(20), (22) and (23) give assuredly equivalent results with the original adjacency matrix. Hence, the dependence of efficiency on grid size N is very useful for the classification of CA rules. Further insight is obtained by using the degree distribution to characterize the CA rules; for example, random and scale-free distributions are found in networks derived from chaotic and complex rules, respectively.

Pairs of the diminished-radix complement of self-complementary rules of ECA and 5TCA are listed in Table 1. Although the individual rules of a pair have different CA patterns, they have similar statistical properties and belong to the same Wolfram class. As indicated by Eq.(25), this correspondence is obvious from the invariance of the time evolution under the exchange of zero and one (complementation).

Networks derived from ECA and 5TCA rules

As shown in Figs.1 and 2, the topology of the derived network reflects properties of the corresponding CA rule. Fig.3 and Fig.4 plots the efficiencies of illustrative ECA and 5TCA rules, respectively. The efficiency values can be categorized into several types. All class I CA have zero efficiency, whereas class III CA are characterized by a high, N -independent efficiency (i.e. short average path length), except for rule 90, 60 and $T42$. For class II CA, the efficiency decreases as N^{-1} , with the exception of rule 184. This N -dependence of class II efficiency can be explained intuitively as follows. Because nontrivial patterns of class II CA are localized, the derived networks are disconnected; hence, the number of edges is proportional to N , whereas the total number of node pairs is proportional to N^2 . Therefore, the contribution of edges to the efficiency decreases as N^{-1} . Although it is somewhat difficult to decide empirically how to classify rule 41, the efficiency values above $N > 1600$ provide evidence that it belongs to class II.

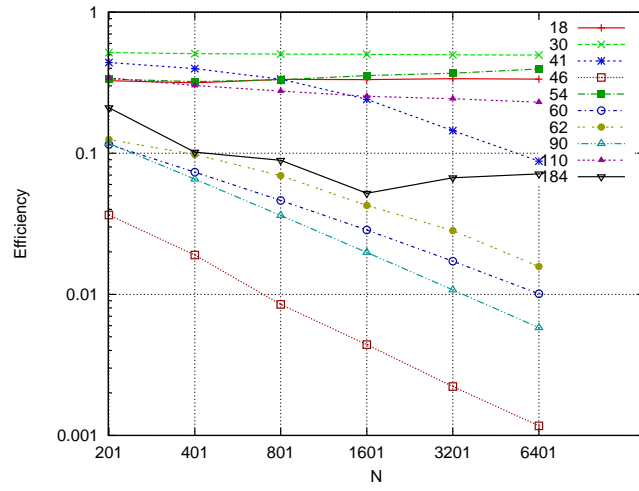


Figure 3: Efficiencies of networks derived from ECA rules, representing the average of ten sampled networks.

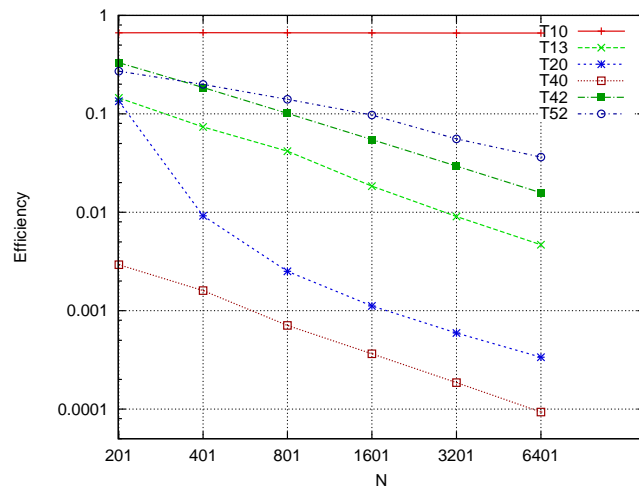


Figure 4: Efficiencies of networks derived from 5TCA rules, representing the average of ten sampled networks.

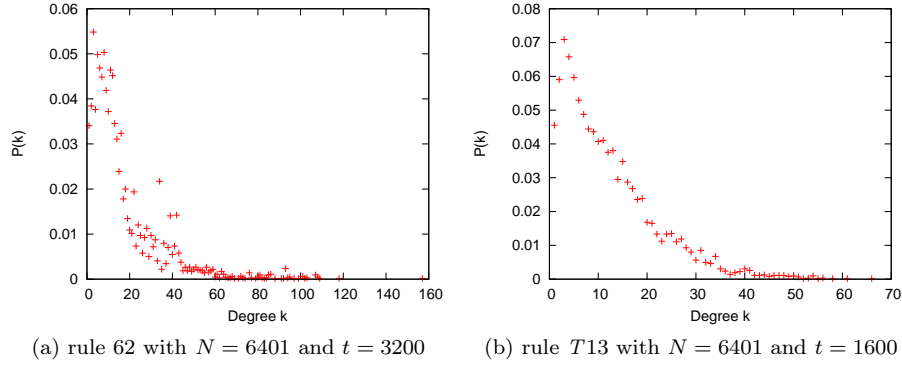


Figure 5: In-degree distributions of networks derived from ECA and 5TCA class II rules.

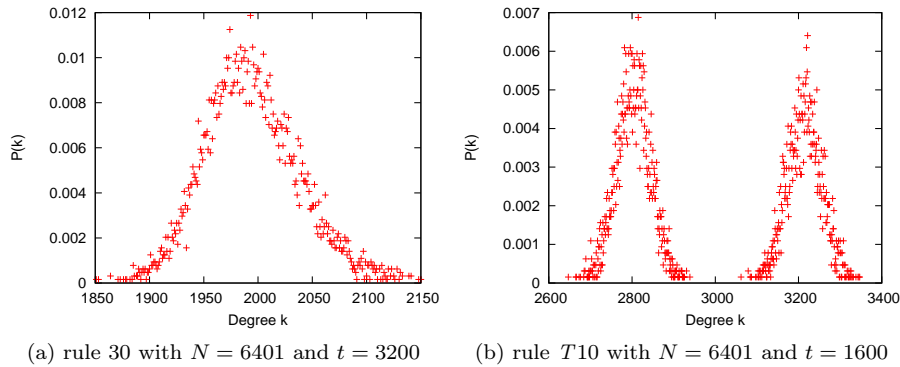


Figure 6: In-degree distributions of networks derived from ECA and 5TCA class III rules.

The efficiency of rule 110 and $T52$, which is thought to belong to class IV, varies as $N^{-0.117}$ and $N^{-0.53}$ (as estimated by least-squares fitting), respectively; these N -dependence indicates that they lie on the “edge of chaos” [19]. In contrast, rule 54 appears to be indistinguishable from class III rules. Furthermore, the efficiency of rule $T20$ is almost proportional to N^{-1} for $N > 1600$. Thus it is difficult to distinguish rule $T20$ from class II rules using only its efficiency dependence.

Rules 90, 60 and $T42$ are exceptional. Because they are additive, each node has the same number of edges, and the total number of edges is proportional to N . Hence, their efficiencies have similar tendencies to those of class II CA. However, in the case of $t = 2^n - 1$ (where n is a positive integer) and $N = 2t + 1$, each node of rule 90 has $2^n = (N - 1)/2$ edges, which means that its numbers of total edges are proportional to N^2 . Consequently, the efficiency of rule 90 oscillates between class II and class III regions. Similar oscillations of the efficiencies of rule 60 and $T42$ are confirmed. Another exception is rule 184, which is usually called the “traffic rule”; its derived network has random values of efficiency, indicating strong dependence on the initial configuration. This random behavior can be interpreted as critical phenomena of the phase transition described in Wolfram [15].

The in-degree distributions of rule 62 and $T13$ (class II) and those of rule 30 and $T10$ (class III) are illustrated in Fig.5 and Fig.6, respectively. Rule 62 is a class II rule but has a large component of class III character [20], which may account for its long-tail distribution. Rule 30 is well-known for its random behavior, from which a random network with a Poisson distribution of degrees is derived. Similarly, rule $T10$ has two peaks, each fitting a Poisson distribution; this double-peak property corresponds to the double-triangle structure of its CA patterns.

Fig.7 shows that class IV rules exhibit exponential decays and long-tail distributions. Fig.8 is an unaveraged distribution of ten sampled networks of rule $T20$, from which we obtain the scale-free exponent $\gamma = 2.096$, based on linear fitting. Hence, a scale-free network can be derived from a class IV rule. However, the N^{-1} efficiency dependence of rule $T20$ suggests that the network derived from rule $T20$ is disconnected in many components, which contrasts with other scale-free networks such as the BA model. We have confirmed that the network derived from rule $T20$ with $N = 6401$ and $t = 1600$ has dozens of disconnected components. In other words, the network can be rendered scale-free and connected by adding, at most, a few dozen edges. By examining Figs.6(b), 7(b) and 7(a), it is apparent that the

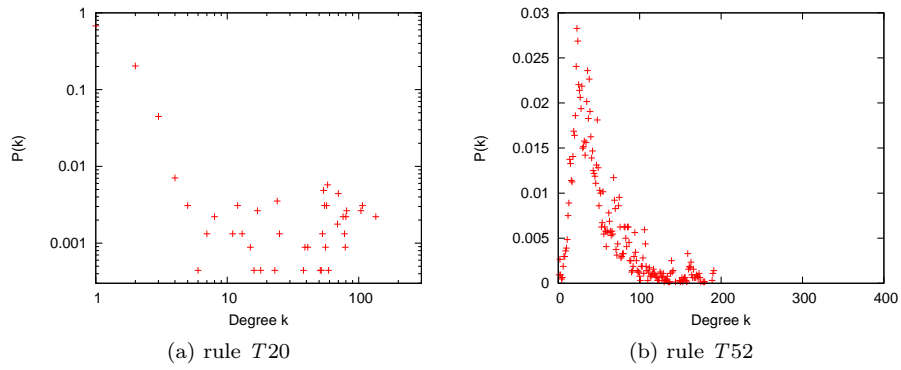


Figure 7: In-degree distributions of networks derived from 5TCA class IV rules with $N = 6401$ and $t = 1600$. (a) The distribution of rule $T20$ plotted on log-log scale exhibits scale-free behavior.

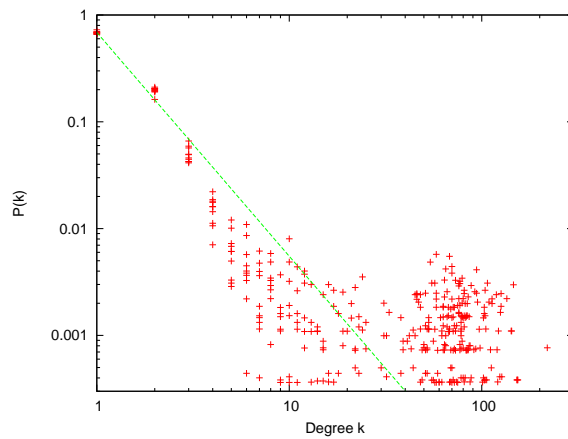


Figure 8: In-degree distribution of networks derived from rule $T20$. The results for ten sampled networks are illustrated with a best-fitting power-law, yielding a scale-free exponent $\gamma = 2.096$.

two peaks gradually collapse; the left peak becomes the scale-free distribution, whereas the right peak becomes a structure at the lower slope. This change of network structure may represent a phase transition from a chaotic phase to a periodic phase.

5. Conclusions and discussion

In this article, we have proposed a method for deriving networks from binary CA rules. Networks of representative ECA and 5TCA rules have been shown and we have discussed their properties in terms of two parameters; their efficiency and their degree distribution. The efficiency parameters appear to be useful in classifying CA rules. Representative degree distributions of complex networks have also been determined, exhibiting Poisson, long-tail and scale-free distributions. Our approach has other interesting aspects, such as a new way to characterize additive rules and the similarity of CA rules. We conclude that our derived network is an effective representation of CA.

A survey of all ECA and 5TCA rules will be reported in a full-length paper. However, our method can be applied or extended to other CA rules. For example, it is straightforward to apply it to binary CA with two or more dimensions and many neighbors, such as the “Game of Life”. The extension of the adjacency matrix to CA with three or more states may yield weighted networks.

One remaining problem is how one is to understand the appearance of a scale-free degree distribution. The fundamental elements leading to emergent scale-free properties are thought to be the growth of the network and the preferential attachment of its links. The former corresponds to the time evolution of CA and the latter may derive from the CA rule and the randomly chosen initial configuration. However, if the following correspondences between dynamical phases of complex systems and types of complex network are assumed,

- Periodic phase \Leftrightarrow disconnected and localized network
- Chaotic phase \Leftrightarrow random network
- Critical phase \Leftrightarrow scale-free network,

it may be possible to describe phase-transition phenomena as evolutions and transformations of network structures. If so, the scale-free network may be an intermediate structure of the description. In any event, these correspondences and the appearance of the scale-free degree distribution warrant further investigation.

Acknowledgments

I wish to acknowledge valuable discussions with Yasumasa Imamura on this topic.

References

- [1] S. Wolfram, *Rev. Mod. Phys.*, **55**, 601 (1983).
- [2] S. Wasserman and K. Faust, *Social Network Analysis* (Cambridge University Press, 1994).
- [3] H. Jeong, B. Tombor, R. Albert, and Z. N. Oltvai, *Nature*, **407**, 651 (2000).
- [4] H. Jeong, S. Mason, A.-L. Barabási, and Z. N. Olivai, *Nature*, **411**, 41 (2001).
- [5] R. Albert, H. Jeong, and A.-L. Barabási, *Nature*, **406**, 378 (1999).
- [6] A.-L. Barabási, R. Albert, and H. Jeong, *Physica A*, **281**, 69 (2000).
- [7] D. J. Watts and S. H. Strogatz, *Nature*, **393**, 440 (1998).
- [8] A.-L. Barabási and R. Albert, *Science*, **286**, 509 (1999).
- [9] D. O’Sullivan, *Environ. Plann. B*, **28**, 687 (2001).
- [10] M. Aldana, *Physica D*, **185**, 45 (2003).
- [11] M. Aldana and P. Cluzel, *Proc. Natl. Acad. Sci.*, **100(15)**, 8710 (2003).

- [12] C. Darabos, M. Giacobini, and M. Tomassini, *Adv. Complex Syst.*, **10**, 85 (2007).
- [13] C. Marr and M.-T. Hütt, *Phys. Lett. A*, **373**, 546 (2009).
- [14] W. Li and N. Packard, *Complex Systems*, **4**, 281 (1990).
- [15] S. Wolfram, *A New Kind of Science* (Wolfram Media, Inc., 2002).
- [16] S. Pemmaraju and S. Skiena, *Computational Discrete Mathematics: Combinatorics and Graph Theory with Mathematica* (Cambridge University Press, 2003).
- [17] V. Latora and M. Marchiori, *Phys. Rev. Lett.*, **87-90**, 198701 (2001).
- [18] S. Boccaletti, V. Latora, Y. Moreno, M. Chavez, and D.-U. Hwang, *Physics Reports*, **424**, 175 (2006).
- [19] C. G. Langton, *Physica D*, **42**, 12 (1990).
- [20] Y. Kayama, H. Anada, and Y. Imamura, *Phys. Lett. A*, **198**, 23 (1995).